Volume 1, Issue 2, pp 1 - 23 year 2024

Journal of the Egyptian Society for Basic Sciences-Physics (JESBSP)

https://jesbsp.journals.ekb.eg/

Hindrance in the preformation probability of the light third particle in collinear ternary fission channels

A. S. Hashem[1, (*)] and W. M. Seif [1, 2]

[1] Cairo University, Faculty of Science, department of Physics, 12613 Giza, Egypt
[2] Joint Institute for Nuclear Research, 141980 Dubna, Russia
(*) **Corresponding author mail:** asayed@sci.cu.edu.eg

Abstract

The preformation probability of the light nucleus generated during the preliminary step of the ternary fission of the heavy ^{252}Cf nucleus is investigated. Considering collinear cluster tripartition kinematics, the relative yields and preformation probabilities of the light ^{4,6}He, ^{10}Be and ^{14}C clusters released in the accompanied ternary fission channels of ^{252}Cf are estimated. Based on the potentials obtained in terms of the Skyrme-SLy4 energy density functionals of the nucleon-nucleon interaction, the Wentzel-Kramers-Brillouin approach is applied to compute the penetration probability of the various nuclei participating in the ternary fission channels. The results demonstrate that the optimal overall excitation energy of the heavy fragments generated in the ternary fission channels is in the region of 3 - 4 MeV. The anticipated probabilities of formation of light nuclei based on collinear configuration are compared to those obtained upon employed the corresponding equatorial arrangement. Calculations using excitation energy greater than the optimal values indicate relatively low preformation probability. As the mass number of emitted light clusters increases, the predicted preformation probabilities decrease exponentially. Generally, the collinear configuration indicates hindrance in both estimated yield and preformation probability, relative to the corresponding equatorial configuration.

Keywords: Preformation probability; Collinear emission; Spontaneous ternary fission; Skyrme interaction

Declarations: The authors have no relevant financial or non-financial interests to disclose.

1. Introduction

Ternary fission is one of the possible decay modes of superheavy nuclei together with binary fission **[1, 2]**. Ternary nuclear fission is most often used to describe the extremely rare process (a few 10^{-3} compared to binary fission) in which a light third fragment is produced along with the two primary fission fragments. It was discovered during both spontaneous and induced fission processes. In most situations of ternary splitting, the lightest fragment is ejected from the "neck" between the two heavy fission fragments and accelerated as a result of two random neck ruptures in the mutual Coulomb field of both fission fragments normal to the binary fission axis. This is referred to as an equatorial ternary fission **[3]**. In other scenarios of ternary fission, the third fragment, together with the other two fragments, is ejected in the direction of the fission axis. This ternary fission mechanism is known as collinear emission **[4-8]**. Oertzen et al. **[9]** observed that the equatorial arrangement is mostly preferred for the ternary fission accompanying light third fragments ^{4}He, ^{10}Be, ^{14}C etc. On the other hand, the collinear arrangement is favored for the heavier outgoing nuclei like ^{48}Ca, ^{50}Ca, ^{54}Ti and ^{60}Cr **[1, 2, 7, 10, 11]**. Nonetheless, true ternary fission of heavy and superheavy nuclei into three fragments of almost similar size would occur only in collinear arrangement **[9]**.

Hamilton et al. **[12]** used Gammasphere with 72 gamma ray detectors to study the cold ternary break up of ^{252}Cf via the triple gamma coincidence technique in the case of ^{4}He, ^{6}He, ^{10}Be and ^{14}C as light third fragments. Ramayya et al. **[13, 14]** measured the isotopic yields for the alpha ternary fission of ^{252}Cf per 100 fission events, with the ternary fission channel ^{103}Zr +^{4}He +^{145}Ba producing the maximum yield. The authors also measured the relative ternary yields of ^{4}He, ^{5,6}He, and ^{10}Be associated with ^{252}Cf fission. α-particles are observed as light particle with the ratio of (2-6)$\times 10^{-3}$ in comparison to binary fission events of ^{240,242}Pu,^{242,244}Cm,^{250,252}Cf, and ^{256,257}Fm fissioning isotopes **[15]**. This ratio falls to 2×10^{-4} for the fissioning $^{243\text{-}248}$Cm isotopes **[16]**. The ^{10}Be particles are observed as emitted light particles **[17-19]** with a relative abundance of roughly 10^{5} to binary spontaneous fission events **[13]**. Ternary fission channels followed by other light nuclei such as ^{5,7}He **[14, 20]**, ^{8}Li **[20]**, and ^{14}C **[12, 21]** were detected with relative ratios of roughly 10^{-4} -10^{-5} to the binary fission events **[16]**. In general, as the mass number of the emitted light particle increases, the relative possibility of ternary fission channels decreases. Ternary heavy fragments such as ^{12}C or even ^{34}Si have been detected with a probability of 2×10^{-4} or 6×10^{-10}, respectively, in spontaneous fission of ^{252}Cf **[18]** relative to binary fission. An island with considerable yields of the collinear cluster tripartition (CCT) of ^{252}Cf was addressed for **[4, 5]** with a light charged particle with mass up to A = 48 (^{48}Ca). Ismail et al. studied the cluster tripartition of ^{260}No in the collinear **[22]** and equatorial **[23]** configurations and investigated the most probable channels with possible light nuclei of even mass numbers A_3 = 4 - 52.

The kinetic energy distribution of alpha particles generated in ternary fission was observed to be mainly Gaussian by Kopach et al. **[20]**. The average kinetic energy of these alpha particles is close to 16 MeV. This energy is essentially greater than the energy released by alpha particles in radioactive alpha decay, leading to longer tracks, that is why ternary alpha particles are commonly referred to as "long range alphas" (LRA). Alvarez et al. **[24]** are the first to discover these long-range alpha particles. The average kinetic energy of the remaining ternary particles, ^{5,6,7}He, ^{8}Li ,^{10}Be and ^{14}C, varies between 8 and 26 MeV **[18, 25]**. Ternary fragmentation of heavy and superheavy nuclei often liberates massive quantities of energy. This released energy mostly contributes to the kinetic and excitation energy of the generated fragments, this results in the production of neutrons and gamma rays in most cases **[26]**. The reaction's Q value is the sum of the total kinetic and total excitation energy of the produced fragments. The overall excitation energy in ternary fragmentation is substantially lower than in binary fragmentation, by roughly 10 MeV in ^{235}U (n^{th}, f) **[27]**. The release of a ternary particle in this manner occurs at an unusual cost to the system's overall excitation energy. The overall excitation energy decreases as the ternary particle gets more kinetic energy **[28]**.

The FOBOS collaboration discovered Collinear Cluster Tripartition CCT with ternary particles with masses $A > 30$ and high yields of roughly 0.5% per fission in both ^{235}U (n^{th}, f) and ^{252}Cf (sf) in 2010 **[5]**. Since the 1940s, most experimental and theoretical studies have agreed that ternary fission is a sequential disintegration with three fragments generated at roughly the same moment. In any case, FOBOS observed that CCT is a successive decay, with three fragments being produced from two perfectly collinear successive binary splittings. Vijayaraghavan et al. **[29]** investigated the kinematics of the fragments produced in CCT using a two-stage splitting technique. The Momentum and energy conservation are used to calculate the kinetic energies of such fission fragments. The breaking of the nucleus into three fragments is predicted to happen in two stages from a hyper-distorted shape. A first neck rupture of the parent radioactive nucleus A occurs during the initial stage producing two fragments (A_1 and A_{CN23}) and finally, the compound nucleus A_{CN23} splits into two fragments, A_2 and A_3 resulting in three fragments. The two subsequent decays' fission axes are completely collinear.

In the present work, we will employ collinear cluster tripartition (CCT) kinematics to theoretically compute the relative yields of ternary fission channels, arising from the fission of ^{252}Cf and experimentally produced by Hamilton et al. **[12]** in the case of ^{4}He, ^{6}He, ^{10}Be and ^{14}C as light third fragments, as a function of the excitation energies of the fragments. Also, we will compute approximate values of the preformation probabilities of the light charged particles inside their compound nuclei at the optimized excitation energies.

2. Theoretical Framework

In collinear emission, the ternary fission of a heavy radioactive nucleus into three fragments takes place in two stages **[29]**. The first stage is a binary fission mechanism in which the original radioactive nucleus A splits into a heavy fragment A_1 and a compound nucleus A_{CN23}. The penetration direction of the first breakup stage is linear, along the horizontal axis connecting the centers of mass of the fissioning nuclei, in view of the conservation law of linear momentum ($\vec{p}_{A_1} = -\vec{p}_{A_{CN23}}$). The second stage is a cluster decay mechanism in which the excited compound nucleus loses its excitation energy as it decays into a medium heavy fragment A_2 and a light cluster A_3. as shown in Fig. 1.

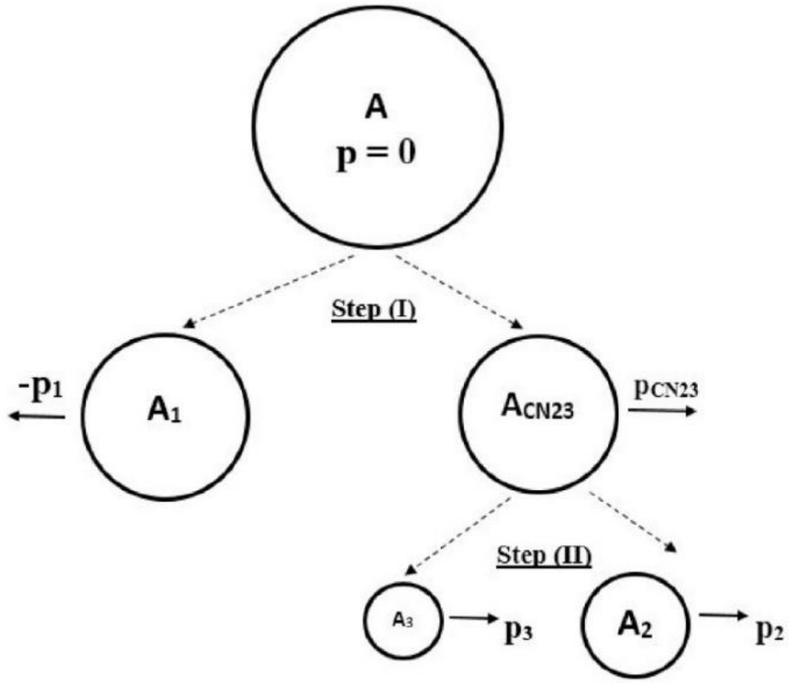

Fig. 1: A schematic representation of a two-step mechanism for ternary fission of a parent nucleus in collinear emission, with the light nucleus (A_3) formed between the two heavy fragments A_1 and A_2 **[30]**.

In general, the energy conservation in the initial stage results in,

$$Q_{1CN23} + E_A^* = KE_1 + E_{A_1}^* + KE_{CN23} + E_{A_{CN23}}^*.$$

where Q_{1CN23} denotes the Q value of the initial stage, the excitation energies of the parent nucleus (A), heavy fragment (A_1), and compound nucleus (A_{CN23}) are denoted as E_A^*, $E_{A_1}^*$ and $E_{A_{CN23}}^*$, respectively. The kinetic energy of the heavy fragment (A_1) and the compound nucleus (A_{CN23}) are denoted by KE_1 and KE_{CN23}, respectively.

Because of the spontaneous decay of the parent nucleus, we have $E_A^* = 0$. The effective emitted energy $Q_{eff1CN23}$ may be determined using the excitation energy of the two heavy nuclei produced in the initial stage ($E_I^* = E_{A_1}^* + E_{A_{CN23}}^*$) and the ground state Q value (Q_{1CN23}) as

$$Q_{eff1CN23} = Q_{1CN23} - E_I^* \quad (1)$$

The conservation of energy in the final step results in,

$$Q_{23} + E_{II}^* + KE_{CN23} = KE_2 + KE_3$$

where Q_{23} and E_{II}^* indicate the Q value and excitation energy in the final stage, respectively. The kinetic energy of the medium heavy fragment (A_2) and light fragment (A_3) are denoted by KE_2 and KE_3, respectively.

$$E_{II}^{*} = E_{A_{CN23}}^{*} - E_{A_2}^{*} - E_{A_3}^{*}$$

The emitted energy in ternary fission (Q_{TF}), deduced from the conservation of energy, can be determined by the summation of the total kinetic ($TKE = \sum_i KE_i$) and excitation $\left(TXE = \sum_i E_{A_i}^{*}\right)$ energies of the three fragments, the compound nucleus' excitation energy completely contributes to the kinetic and excitation energies of the medium heavy and light fragments A_2 and A_3.

$$Q_{TF} = TKE + TXE. \tag{2}$$

The evaluation of the total interaction potential between the heavy fragment A_1 and the compound nucleus A_{1CN23}, as well as between the medium heavy fragment A_2 and the light nucleus A_3, is critical in the calculation of the penetration probabilities in stages (I) and (II), as well as the relative yield in ternary fission. We will employ the energy density functional theory using the Skyrme–Hartree–Fock (Skyrme–HF) formalism **[31, 32]** to calculate the binding energy and interaction potential between two nuclei. The overall binding energy of a nucleus can be represented as the integral of the energy density functional **[31, 33]**.

$$E = \int H d\vec{r} \tag{3}$$

The kinetic, nuclear interaction, and Coulomb interaction energy portions are all included in the energy density functional H,

$$H = \frac{\hbar^2}{2m}\left[\tau_p(\vec{r}) + \tau_n(\vec{r})\right] + H_{sky}(\vec{r}) + H_{coul}(\vec{r}) \tag{4}$$

The effective-mass form factor **[34]** in the kinetic energy portion is obtained by

$$f_i(\vec{r}) = 1 + \frac{2m}{\hbar^2}\left\{\frac{1}{4}\left[t_1\left(1+\frac{x_1}{2}\right) + t_2\left(1+\frac{x_2}{2}\right)\right]\rho(\vec{r}) + \frac{1}{4}\left[t_2\left(x_2+\frac{1}{2}\right) - t_1\left(x_1+\frac{1}{2}\right)\right]\rho_i(\vec{r})\right\} \tag{5}$$

the kinetic energy densities for protons ($i = p$) and neutrons ($i = n$) are obtained by

$$\tau_i(\vec{r}) = \frac{3}{5}(3\pi^2)^{\frac{2}{3}}\rho_i^{\frac{5}{3}} + \frac{1}{36}\frac{(\vec{\nabla}\rho_i)^2}{\rho_i} + \frac{1}{3}\Delta\rho_i + \frac{1}{6}\frac{\vec{\nabla}\rho_i.\vec{\nabla}f_i + \rho_i\Delta f_i}{f_i} - \frac{1}{12}\rho_i\left(\frac{\vec{\nabla}f_i}{f_i}\right)^2 + \frac{1}{2}\rho_i\left(\frac{2m}{\hbar^2}\frac{W_0}{2}\frac{\vec{\nabla}(\rho+\rho_i)}{f_i}\right)^2 \tag{6}$$

where ρ_i indicates the proton ($i = p$) or neutron ($i = n$) density of the nucleus and $\rho = \rho_p + \rho_n$, W_0 indicates the Skyrme spin–orbit interaction's strength. The Skyrme nuclear interaction portion H_{sky} is given by

$$H_{sky}(\vec{r}) = \frac{t_0}{2}\left[\left(1+\frac{x_0}{2}\right)\rho^2 - \left(x_0+\frac{1}{2}\right)(\rho_p^2+\rho_n^2)\right] + \frac{1}{12}t_3\rho^{\alpha}\left[\left(1+\frac{x_3}{2}\right)\rho^2 - \left(x_3+\frac{1}{2}\right)(\rho_p^2+\rho_n^2)\right] + \frac{1}{4}\left[t_1\left(1+\frac{x_1}{2}\right)+t_2\left(1+\frac{x_2}{2}\right)\right]\tau\rho + \frac{1}{4}\left[t_2\left(x_2+\frac{1}{2}\right)-t_1\left(x_1+\frac{1}{2}\right)\right](\tau_p\rho_p+\tau_n\rho_n) + \frac{1}{16}\left[3t_1\left(1+\frac{x_1}{2}\right)-t_2\left(1+\frac{x_2}{2}\right)\right](\nabla\rho)^2 - \frac{1}{16}\left[3t_1\left(x_1+\frac{1}{2}\right)+t_2\left(x_2+\frac{1}{2}\right)\right]\left[(\nabla\rho_n)^2+(\nabla\rho_p)^2\right] - \frac{W_0^2}{4}\frac{2m}{\hbar^2}\left[\frac{\rho_p}{f_p}(2\nabla\rho_p+\nabla\rho_n)^2+\frac{\rho_n}{f_n}(2\nabla\rho_n+\nabla\rho_p)^2\right] \quad (7)$$

where t_0, t_1, t_2, t_3, x_0, x_1, x_2, x_3, and α denote the Skyrme Sly4-force parameters **[35]**. The Coulomb energy density can be calculated by adding the direct and exchange components, the second term is considered in the Slater approximation **[36, 37]**,

$$H_{Coul}(\vec{r}) = \frac{e^2}{2}\rho_p(\vec{r})\int\frac{\rho_p(\vec{r'})}{|\vec{r}-\vec{r'}|}d\vec{r'} - \frac{3e^2}{4}\left(\frac{3}{\pi}\right)^{1/3}\left(\rho_p(\vec{r})\right)^{4/3} \quad (8)$$

In the present work, we consider the neutron and proton density distributions of a nucleus to be spherical symmetric Fermi functions,

$$\rho_i(\vec{r}) = \frac{\rho_{0i}}{1+exp\left(\frac{r-R_{0i}}{a_i}\right)}, i = \{n,p\} \quad (9)$$

To preserve the overall neutron and proton numbers, the neutron and proton densities are normalized using $\rho_{0n(p)}$, $\int \rho_{n(p)}(\vec{r})d\vec{r} = N(Z)$, of each nucleus. The half density radius R_{0i} and diffuseness a_i can be calculated using the formulae **[38]**,

$$\begin{aligned} R_{0n}(fm) &= 0.953(N)^{\frac{1}{3}} + 0.015(Z) + 0.774, \\ R_{0p}(fm) &= 1.322(Z)^{\frac{1}{3}} + 0.007(N) + 0.022, \\ a_n(fm) &= 0.446 + 0.072\left(\frac{N}{Z}\right), \\ a_p(fm) &= 0.449 + 0.071\left(\frac{Z}{N}\right) \end{aligned} \quad (10)$$

The nuclear and Coulomb interaction potentials between any two nuclei are provided by

$$V_N(R) + V_C(R) = E_{tot}(R) - E_1 - E_2 \quad (11)$$

where $E_{tot}(R)$ denotes the total nuclear interaction energy of a system of two nuclei, E_1 and E_2 denotes the binding energies of the two nuclei 1 and 2 defined by Eq. (3) respectively.

$$E_{tot}(R) = \int H\left[\rho_{1p}(\vec{r}) + \rho_{2p}\left(\vec{r} - \vec{R}\right), \rho_{1n}(\vec{r}) + \rho_{2n}\left(\vec{r} - \vec{R}\right)\right] d\vec{r}. \qquad (12)$$

The sum of the nuclear, Coulomb, and centrifugal potentials yields the total interaction potential

$$V(R) = \lambda V_N(R) + V_C(R) + V_{cent}(R). \qquad (13)$$

The Langer formulation of centrifugal potential **[39]** can be evaluated as

$$V_{cent}(R) = \frac{(\ell+1/2)^2\hbar^2}{2\mu R^2}. \qquad (14)$$

Where $\mu = \frac{m_1 m_2}{m_1+m_2}$ refers to the reduced mass of the two interacting nuclei. The renormalization factor λ in Eq. (13) can be calculated using the Bohr-Sommerfeld quantization rules **[40, 41]**,

$$\int_{R_1}^{R_2} k(r) d\vec{r} = (2n+1)\frac{\pi}{2}. \qquad (15)$$

Here, $k(r) = \sqrt{2\mu|V(r) - Q|/\hbar^2}$, and the quantum number n denotes the number of internal nodes in the binary system's quasibound radial wave function. We use the Bohr-Sommerfeld quantization rule, with $n = 0$ being the smallest quantum number obeying the Pauli exclusion principle.

The semiclassical Wentzel-Kramers-Brillouin (WKB) approach **[42, 43]** can be used to evaluate the penetration probability in stage (I),

$$P_{1CN23} = exp\left\{-\frac{2}{\hbar}\int_{R_{2(1CN23)}}^{R_{3(1CN23)}} \left[2\mu_{1CN23}\left(V_{1CN23}(r) - Q_{eff1CN23}\right)\right]^{1/2} dr\right\} \qquad (16)$$

where V_{1CN23} is the total interaction potential between the heavy fragment A_1 and the compound nucleus A_{CN23}, $Q_{eff1CN23}$ is defined in Eq. (1), the three classical turning points $R_i(i = 1-3)$ in equations (15) and (16), in femtometers, are obtained by $V_{1CN23}(R_i) = Q_{eff1CN23}$.

Due to the absence of any observed value for the kinetic energy of the emitted light cluster A_3 in collinear (polar) emission, a value of about half the observed average value of the light cluster kinetic energy in the equatorial maximum of emission **[44]** is used to calculate the penetration probability in stage (II) of the collinear configuration because the light cluster in the collinear emission interacts with only one heavy nucleus (A_2) while in equatorial configuration it interacts with the two heavy fragments A_1 and A_2. This value is obtained in terms of the average height of the interaction potentials of the light cluster in the different collinear fragmentation channels, to give the same ratio of the observed light cluster kinetic energy in the equatorial emission relative to the average height of its potentials with A_1 and A_2. Hence, the penetration probability in stage (II) is given as

$$P_{23} = exp\left\{-\frac{2}{\hbar}\int_{R_{2(23)}}^{R_{3(23)}} \left[2\mu_{23}\left(V_{23}(r) - 0.5\, KE_{3exp}\right)\right]^{1/2} dr\right\} \qquad (17)$$

where V_{23} is the total interaction potential between the medium heavy fragment A_2 and a light cluster A_3, KE_{3exp} is the experimental kinetic energy of the light cluster in equatorial configuration, the three classical turning points $R_i(i = 1 - 3)$ in equations (15) and (17), in femtometers, are obtained by $V_{23}(R_i) = 0.5\ KE_{3exp}$.

The relative yield of a given ternary fission channel ($A_{1,2,3}$) can be calculated in terms of the total penetration probability of collinear ternary fission ($P_{TF} = P_{1CN23} \times P_{23}$ **[11]**), and the penetration probability of the corresponding binary fission of the parent nucleus P_{BF} **[44]** as,

$$Y_{cal} = \frac{S_3\, P_{TF}}{P_{BF}} \tag{18}$$

The preformation probability of the emitted cluster in ternary fission can be obtained as **[44]**,

$$S_3 = \frac{Y_{cal}(without\ S_3)}{Y_{exp}} \tag{19}$$

where Y_{exp} is the experimental relative yield **[12, 13, 17, 21, 45]** in ternary fission.

3. Results and Discussion

We explore the kinematics of the collinear ternary fission of the spontaneously fissioning ^{252}Cf nucleus as two stages in this paper. Based on the Skyrme-SLy4 model of the *NN* force, the energy density formalism is utilized to compute the interaction potential between the heaviest nucleus and the intermediate compound nucleus (V_{1CN23}) generated in stage I, as well as the interaction potential between the second heavy nucleus and the light released nucleus (V_{23}). The relative yields of the practically obtained ternary fission channels are then computed compared to the equivalent binary fission, using the penetration probability of the nuclei included in each step. The effect of the nuclei's excitation energy in the ternary fission process on the preformation probability of the produced light particle is investigated, to gain more information on the anticipated preformation probability at the optimal values of the excitation energy. We concentrate on the reported channels of ^{252}Cf ternary fission modes, which comprise ^{4,6}He, ^{10}Be, and ^{14}C nuclei as light particles **[1, 2, 12, 13, 17, 21, 45]**.

Table I displays the predicted relative yields of the several obtained channels of ternary fission of ^{252}Cf (column 1), with the ^{4}He nucleus representing the light particle. In the second column of Table I, the relative experimental yields obtained for the reported 16 channels per 100 fission processes are listed. As shown in Table I, the heaviest nucleus mass number ranges between A_1 = 132 for ^{132}Sn and A_1 = 156 for ^{156}Nd, whereas the corresponding medium heavy nucleus mass number ranges between A_2 = 116 for ^{116}Pd and A_2 = 92 for ^{92}Kr. The ternary channels (^{145}Ba + ^{103}Zr + ^{4}He) and (^{147}Ba + ^{101}Zr + ^{4}He) have the highest relative yields of 0.084% and 0.082% respectively. An example for the radial dependence of the total mutual interaction potentials between the participating nuclei is shown in Fig. (2) for the ^{252}Cf (A_1 = ^{145}Ba, A_2 = ^{103}Zr, A_3 =^{4}He) ternary fission channel. All of the existing practical data on ternary fission, including relative yield and kinetic energy, are arithmetic average, and their highest values are generally associated with equatorial configuration. Columns 3(7) and 5(9) show the computed relative yields with excitation energy of preceding step (I) E^*_I = 3 MeV, equivalent to E^*_{A1} = 1.5 MeV and E^*_{ACN23} = 1.5 MeV, and E^*_I = 4 MeV, equivalent to E^*_{A1} = 2 MeV and E^*_{ACN23} = 2 MeV, for the collinear and equatorial ternary fission configurations respectively. The practical kinetic energy of the released light particle (KE_{3exp}) is utilized to compute P_{23} penetration probability **[1, 2, 12, 13, 17, 21, 45]**. The kinetic energy of the released particles follows a Gaussian shape, with the largest yield occurring at 15.7 MeV. Columns 4(8) and 6(10) of Table I show the calculated preformation probability of the α particle for the listed channels, as determined by comparing the computed yields Y_{cal} (E^*_I = 3 MeV) and Y_{cal} (E^*_I = 4 MeV) with the experimental results for the ^{4}He-accompanied ternary fission channels of ^{252}Cf based on collinear and equatorial configurations respectively. For the collinear emission, the extracted values of S_α (E^*_I = 3 MeV) lies between 5.21×10^{-6} and 3.05×10^{-3}, with an average value of 2.44×10^{-4}. The estimated values of S_α (E^*_I = 4 MeV) ranges between 6.08×10^{-7} and 3.83×10^{-4}, with a smaller average value of 3.06×10^{-5}. For the equatorial emission, the S_α values for E^*_I = 4 MeV range from 0.001 to 0.013, with a mean value of 0.004. The α-particle preformation probability for E^*_I = 3 MeV spans between S_α = 0.004 and S_α = 0.093, with an overall average of approximately 0.031. It is evident from the above discussion that the values of α preformation probability for ternary fission of ^{252}Cf based on collinear configuration have then lower order of magnitude than that extracted based on the equatorial configuration. This leads us to the result that equatorial configuration is most favored for α emission since it gives higher yield and higher preformation probability for all the listed observed channels in Table I.

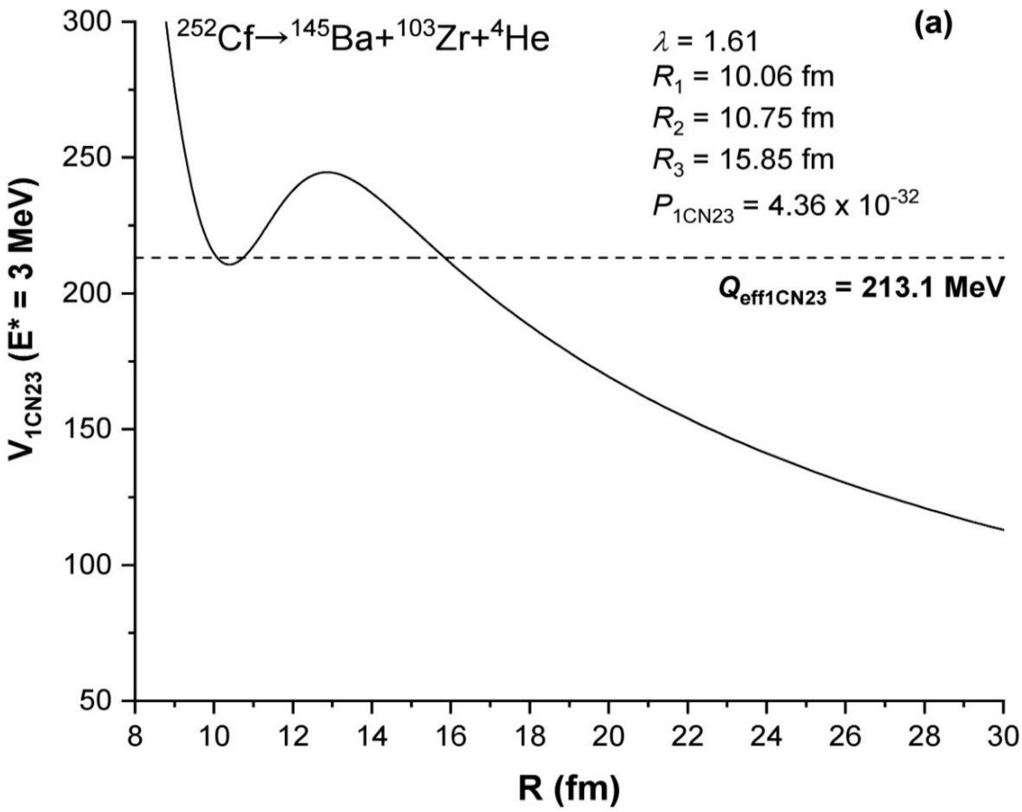

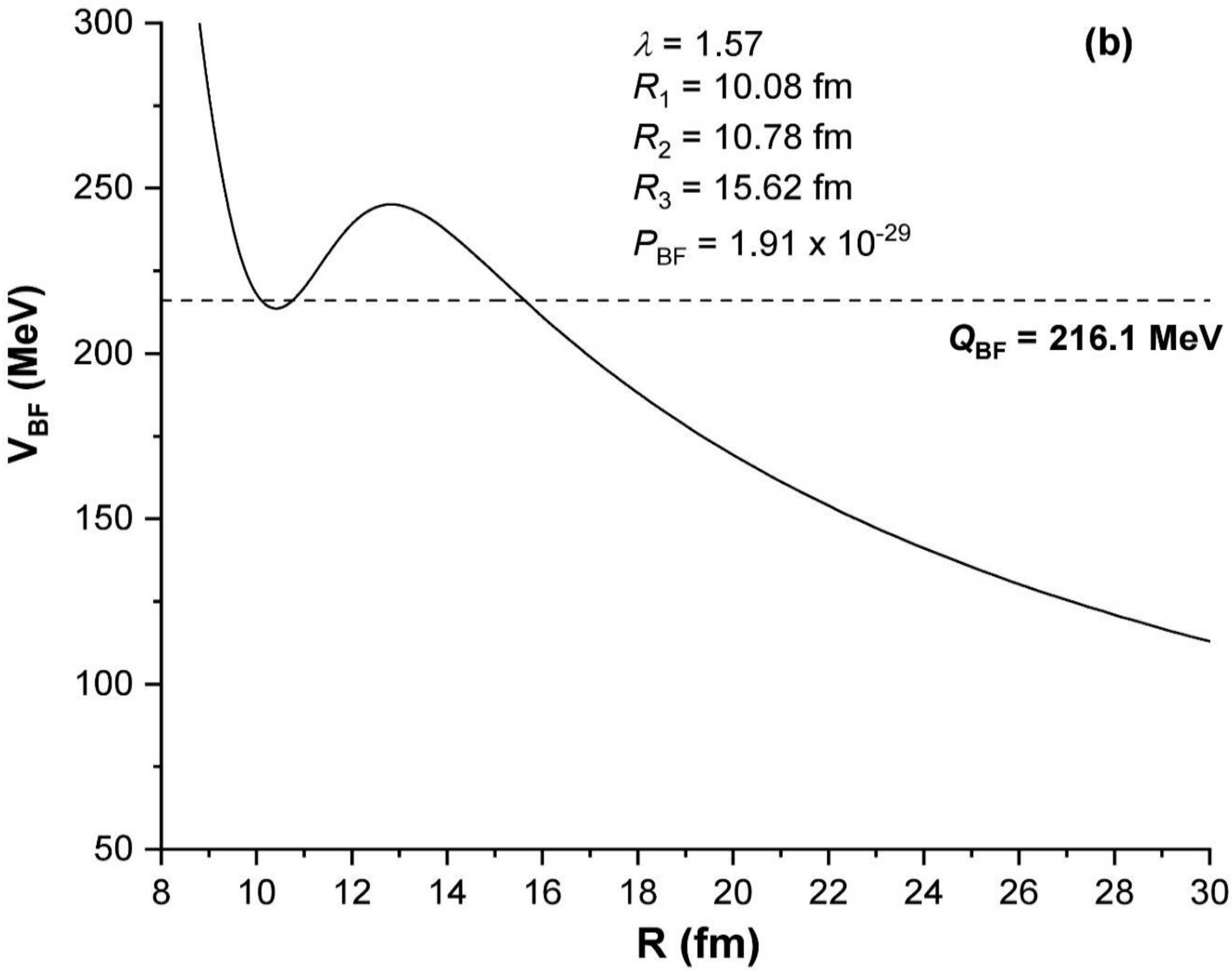
λ = 1.57
R1 = 10.08 fm
R2 = 10.78 fm
R3 = 15.62 fm
PBF = 1.91 x 10-29
(b)
QBF = 216.1 MeV
VBF (MeV)
R (fm)
300
250
200
150
100
50
8
10
12
14
16
18
20
22
24
26
28
30

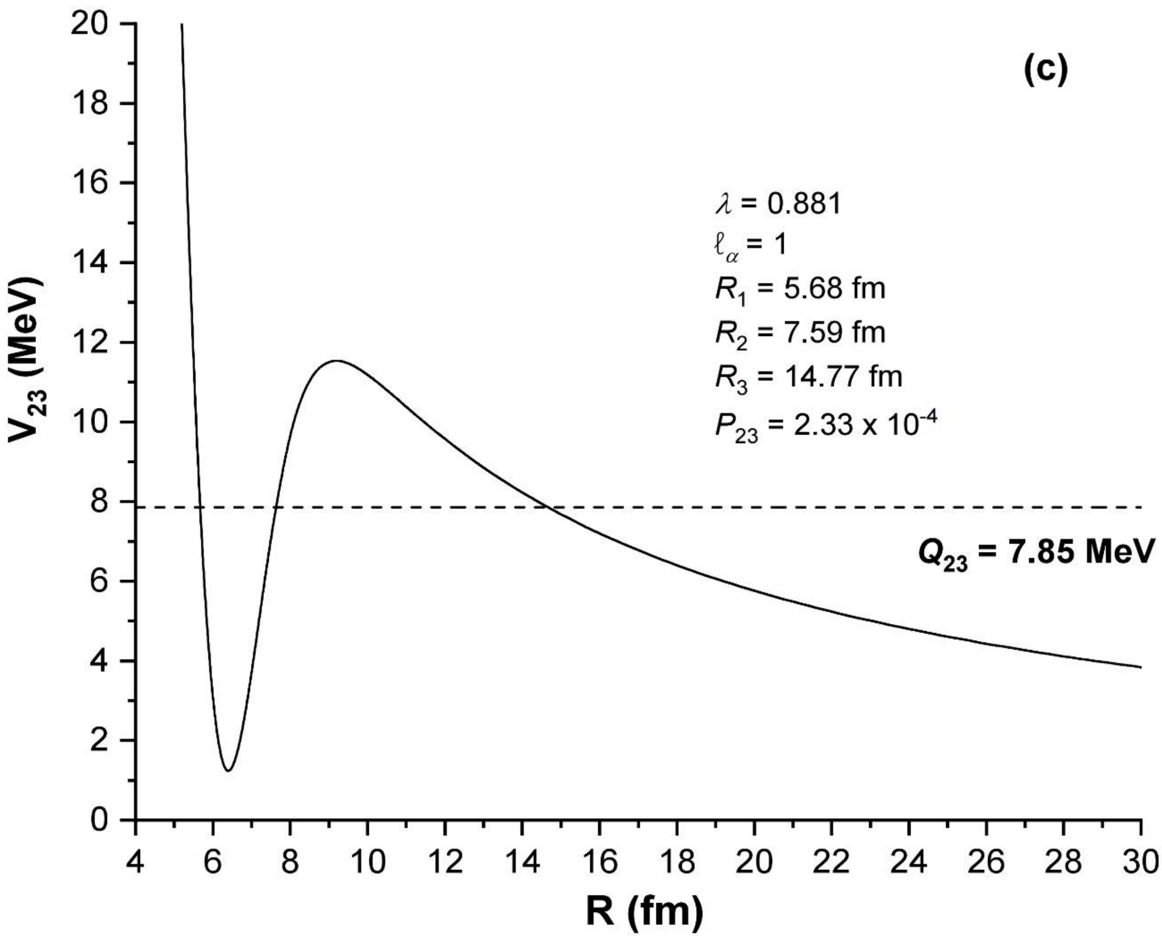

Fig. 2: The radial dependencies of the total potentials (a) V_{1CN23} (E^*_{I} = 3 MeV) (^{145}Ba, ^{107}Mo), (b) V_{BF} (^{145}Ba, ^{107}Mo), and (c) V_{23} (^{103}Zr, ^{4}He) which take part in the ternary fission path ^{252}Cf (A_1 = ^{145}Ba, A_2 = ^{103}Zr, A_3 = ^{4}He), using the NN interaction of Skyrme-SLy4. On each panel, the turning points ($R_{1,2,3}$) related to each pair of nuclei and the normalizing coefficient λ (Eq. (13)) determined from the Bohr-Sommerfeld quantization rule are shown. The α-particle (^{4}He) centrifugal potential of the lowest angular momentum quantum number and yielding three turning points is investigated.

JESBSP volume 1, issue 2, pp 1 – 23, year 2024

\\

Table I: Preformation probabilities of α particles for the detected α-accompanied ternary fission channels of ^{252}Cf, obtained by the comparison of the experimental relative yield (Y_{exp}) with the predicted relative yield (Y_{cal}) at step (I) excitation energy of E^*_I (E^*_{A1}, E^*_{ACN23}) = 3 MeV and 4 MeV, taking into account collinear (Q_{23} = 7.85 MeV) and equatorial (Q_{23} = 15.7 MeV) arrangements of the ternary system.

Ternary fission Channel	Y_{exp}	**Collinear (Q_{23} = 7.85 MeV)**				**Equatorial (Q_{23} = 15.7 MeV) [44]**			
		E^*_I = 3 MeV		E^*_I = 4 MeV		E^*_I = 3 MeV		E^*_I = 4 MeV	
		Y_{cal}	S_α	Y_{cal}	S_α	Y_{cal}	S_α	Y_{cal}	S_α
$^{156}Nd+^{92}Kr+^{4}He$	2.00×10^{-3}	6.10×10^{-6}	3.05×10^{-3}	7.66×10^{-7}	3.83×10^{-4}	1.85×10^{-4}	9.26×10^{-2}	2.33×10^{-5}	1.16×10^{-2}
$^{152}Ce+^{96}Sr+^{4}He$	8.00×10^{-3}	1.72×10^{-6}	2.15×10^{-4}	2.10×10^{-7}	2.62×10^{-5}	1.86×10^{-4}	2.32×10^{-2}	2.34×10^{-5}	2.93×10^{-3}
$^{150}Ce+^{98}Sr+^{4}He$	1.40×10^{-2}	1.96×10^{-6}	1.40×10^{-4}	2.44×10^{-7}	1.74×10^{-5}	5.52×10^{-4}	3.94×10^{-2}	6.86×10^{-5}	4.90×10^{-3}
$^{149}Ce+^{99}Sr+^{4}He$	1.80×10^{-2}	1.48×10^{-6}	8.22×10^{-5}	1.76×10^{-7}	9.77×10^{-6}	4.91×10^{-4}	2.73×10^{-2}	5.84×10^{-5}	3.24×10^{-3}
$^{148}Ce+^{100}Sr+^{4}He$	2.10×10^{-2}	2.05×10^{-6}	9.74×10^{-5}	2.51×10^{-7}	1.20×10^{-5}	1.87×10^{-4}	8.90×10^{-3}	2.29×10^{-5}	1.09×10^{-3}
$^{148}Ba+^{100}Zr+^{4}He$	3.80×10^{-2}	5.10×10^{-7}	1.34×10^{-5}	6.20×10^{-8}	1.63×10^{-6}	3.09×10^{-4}	8.12×10^{-3}	3.75×10^{-5}	9.88×10^{-4}
$^{147}Ce+^{101}Sr+^{4}He$	1.40×10^{-2}	1.48×10^{-6}	1.06×10^{-4}	1.71×10^{-7}	1.22×10^{-5}	1.60×10^{-4}	1.14×10^{-2}	1.85×10^{-5}	1.32×10^{-3}
$^{147}Ba+^{101}Zr+^{4}He$	8.20×10^{-2}	4.27×10^{-7}	5.21×10^{-6}	5.15×10^{-8}	6.28×10^{-7}	3.05×10^{-4}	3.71×10^{-3}	3.67×10^{-5}	4.48×10^{-4}
$^{146}Ba+^{102}Zr+^{4}He$	9.00×10^{-3}	6.61×10^{-7}	7.34×10^{-5}	8.55×10^{-8}	9.50×10^{-6}	3.81×10^{-4}	4.23×10^{-2}	4.92×10^{-5}	5.47×10^{-3}
$^{145}Ba+^{103}Zr+^{4}He$	8.40×10^{-2}	5.33×10^{-7}	6.34×10^{-6}	6.73×10^{-8}	8.02×10^{-7}	3.60×10^{-4}	4.29×10^{-3}	4.56×10^{-5}	5.43×10^{-4}
$^{144}Ba+^{104}Zr+^{4}He$	1.70×10^{-2}	7.70×10^{-7}	4.53×10^{-5}	1.02×10^{-7}	6.01×10^{-6}	4.21×10^{-4}	2.48×10^{-2}	5.59×10^{-5}	3.29×10^{-3}
$^{142}Xe+^{106}Mo+^{4}He$	1.80×10^{-2}	2.17×10^{-7}	1.21×10^{-5}	2.94×10^{-8}	1.63×10^{-6}	2.89×10^{-4}	1.61×10^{-2}	3.91×10^{-5}	2.17×10^{-3}
$^{141}Xe+^{107}Mo+^{4}He$	3.00×10^{-2}	2.21×10^{-7}	7.37×10^{-6}	2.96×10^{-8}	9.87×10^{-7}	2.86×10^{-4}	9.54×10^{-3}	3.84×10^{-5}	1.28×10^{-3}
$^{140}Xe+^{108}Mo+^{4}He$	7.00×10^{-3}	2.81×10^{-7}	4.02×10^{-5}	4.04×10^{-8}	5.78×10^{-6}	3.54×10^{-4}	5.06×10^{-2}	5.09×10^{-5}	7.28×10^{-3}
$^{136}Te+^{112}Ru+^{4}He$	1.10×10^{-2}	9.94×10^{-8}	9.04×10^{-6}	1.54×10^{-8}	1.40×10^{-6}	6.80×10^{-4}	6.18×10^{-2}	1.05×10^{-4}	9.59×10^{-3}
$^{132}Sn+^{116}Pd+^{4}He$	6.00×10^{-3}	3.60×10^{-8}	6.01×10^{-6}	6.15×10^{-9}	1.02×10^{-6}	4.55×10^{-4}	7.58×10^{-2}	7.75×10^{-5}	1.29×10^{-2}

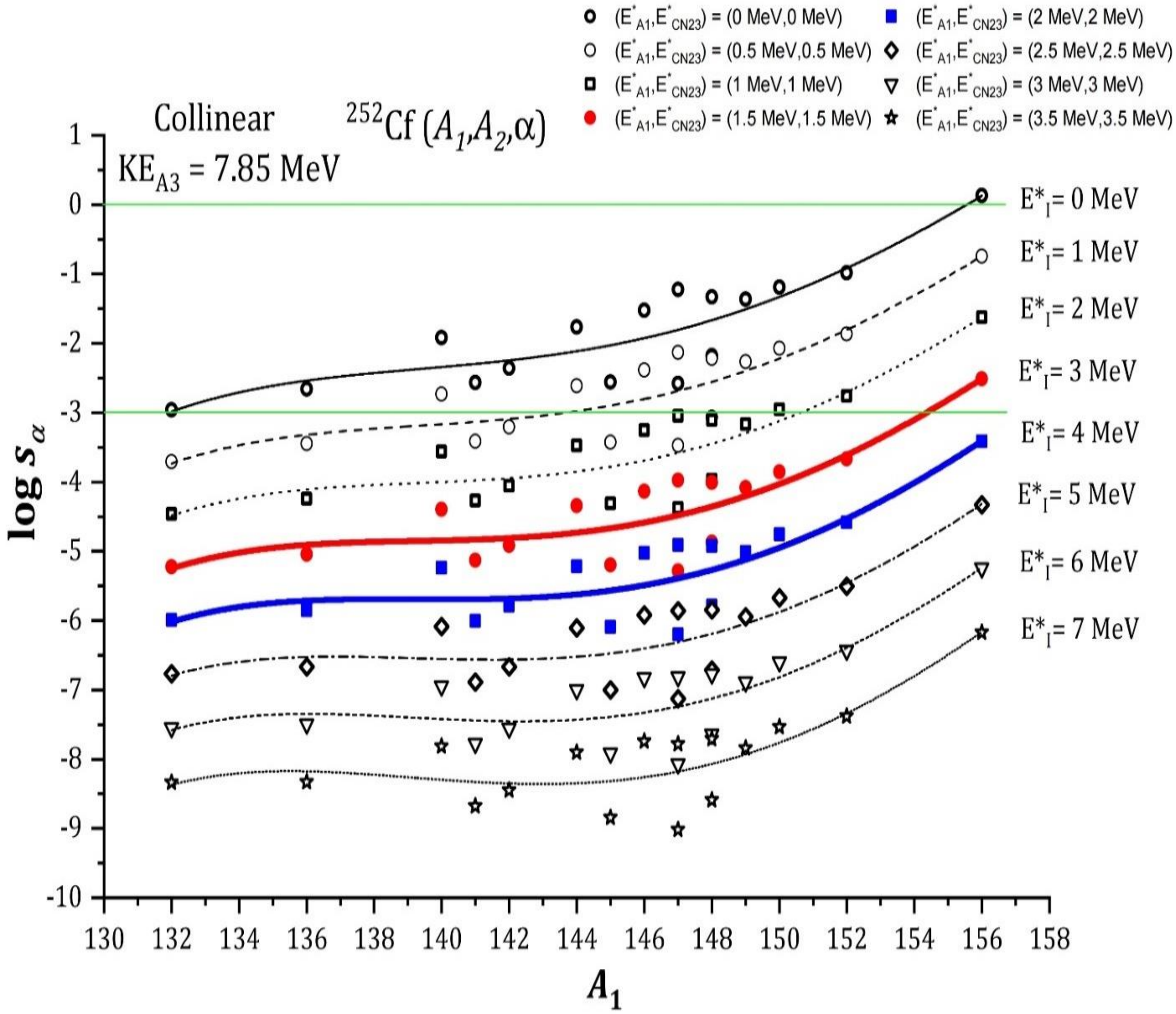

Fig. 3: The dependence of the logarithm of the preformation probability of α particles on the heaviest nucleus mass number (A_1) for the ^{252}Cf accompanied α-ternary fission channels in collinear configuration, evaluated for different excitation energies of step (I) E^*_I (E^*_{A1}, E^*_{ACN23}) = 0 − 7 MeV with Q_{23} = 7.85 MeV. Continuous, dashed and dotted curves are drawn to direct the viewer's attention.

Fig. (3) displays the dependence of the logarithm of the preformation probability of α particles on the heaviest nucleus mass number (A_1) for the ^{252}Cf accompanied α-ternary fission channels in collinear configuration, evaluated for different excitation energies of step (I) E^*_I (E^*_{A1}, E^*_{ACN23}) = 0 − 7 MeV where E^*_I is divided evenly among A_1 as well as A_{CN23}, using Q_{23} = 0.5 $KE_{\alpha exp}$ = 7.85 MeV. The continuous, dashed and dotted curves are drawn to direct the viewer's attention. As seen in Fig. (3), raising the excitation energy E^*_I reduces the anticipated preformation probability as a result of lowering the predicted relative yield. Based on E^*_I = 3 - 4 MeV computations for equatorial configuration **[44]**, the expected S_α for the nuclei in the vicinity of the participating heavy nuclei is within the range of 10^{-2} - 10^{-3}. The maximum recognized excited states of the A_1 fragments involved in the reported channels is 2.304 MeV

(^{148}Ba ($J = 12^+$)) and 7.244 MeV (^{132}Sn ($J = 7$)) **[46]**. While for the collinear configuration, an extremely small values of S_α less than 10^{-3} based on E^*_I = 3 - 4 MeV and higher. This enhances the preference of the equatorial configuration over the collinear configuration for the released α-particles in ternary fission of ^{252}Cf. In the reported ternary fission channels of ^{252}Cf, the Q-value of the quasi-fission process providing the binary $A_1 + A_{CN23}$ structure is typically higher than that generating the binary $A_2 + A_{CN13}$ structure **[47]** in the first stage of collinear emission. This confirms the hypothesis of formation of the released light particle on the surface of the A_{CN23} ($A_2 + A_3$) composite structure **[44]**.

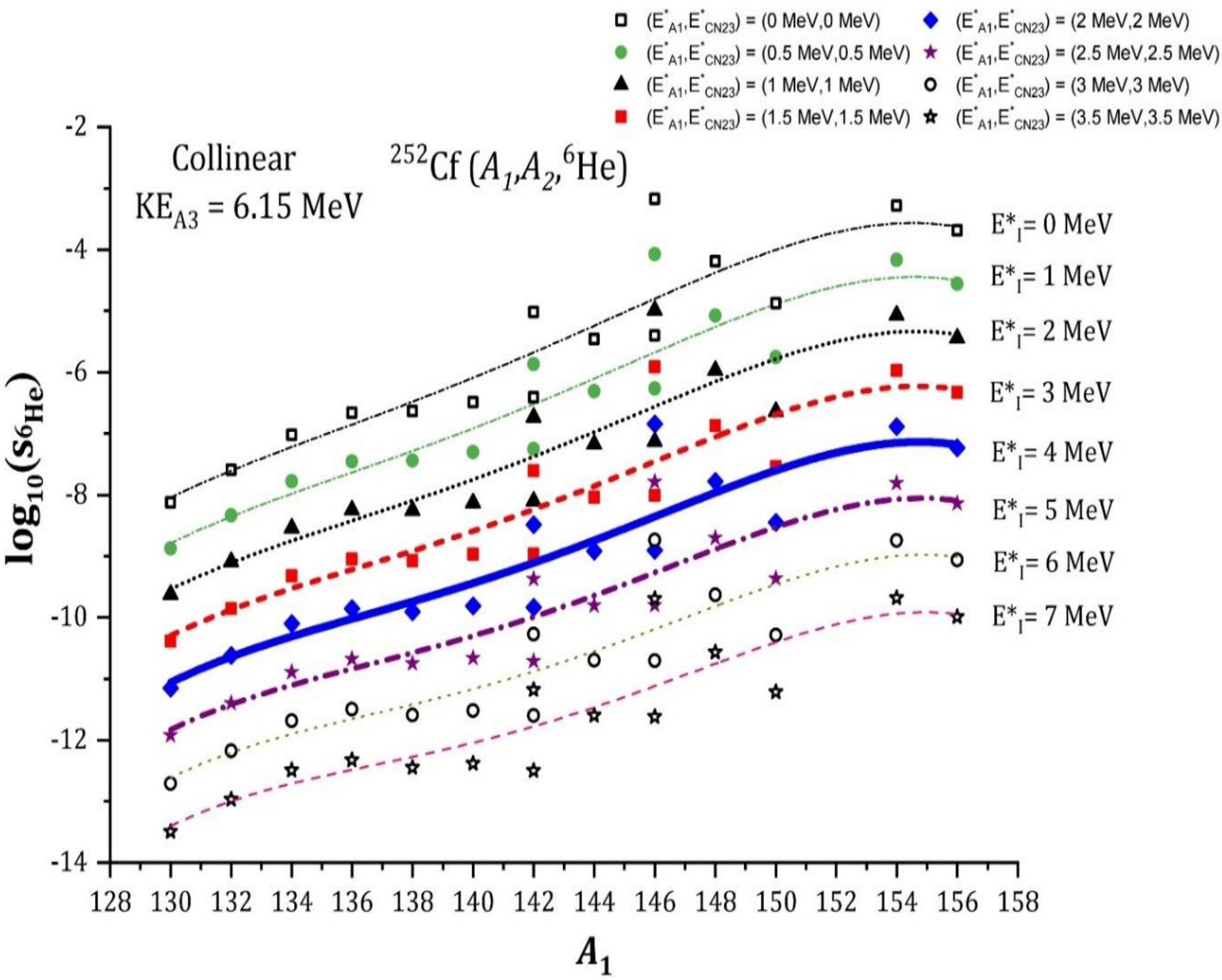

Fig. 4: The dependence of the logarithm of the preformation probability of ^{6}He particles on the heaviest nucleus mass number (A_1) for the ^{252}Cf accompanied ^{6}He-ternary fission channels in collinear configuration, evaluated for different excitation energies of step (I) E^*_I (E^*_{A1}, E^*_{ACN23}) = 1 − 7 MeV with Q_{23} = 6.15 MeV. Continuous, dashed and dotted curves are drawn to direct the viewer's attention.

The ^{6}He nucleus is the first heavier cluster than ^{4}He detected as the released third cluster in the ternary break up of ^{252}Cf. There are fifteen ^{6}He accompanied ternary fission channels of ^{252}Cf. Table II lists these channels and their relative experimental yields in columns 1 and 2 respectively. The ternary fission channels (^{138}Xe + ^{108}Mo + ^{6}He) and (^{150}Ce + ^{96}Sr + ^{6}He) produce the highest relative experimental yield percentage of about 0.03% and 0.021% respectively. The detected emission peaks at around 12.3 MeV for ^{6}He kinetic energy in the equatorial configuration. Fig. (4) displays the dependence of the logarithm of the preformation probability of ^{6}He particles (log (S_{6He})) on the heaviest nucleus mass number (A_1) for the ^{6}He-accompanied ternary fission channels of ^{252}Cf in collinear configuration, evaluated for different excitation energies of step (I) E^*_I (E^*_{A1}, E^*_{ACN23}) = 1 − 7 MeV with Q_{23} = 0.5 KE_{3exp} = 6.15 MeV. The continuous, dashed, and dotted curves are drawn in Fig. (4) to direct the viewer's attention. According to Fig. (4), raising the excitation energy E^*_I (E^*_{A1}, E^*_{ACN23}) reduces the predicted preformation probability values. The computations corresponding to E^*_I = 1 MeV will result in a mean value of S_{6He} in the order of 10^{-2} and 10^{-6} for equatorial and collinear configurations respectively. In both equatorial and collinear configurations, raising the stage (I) excitation energy to 2, 3, and 4 MeV reduces the order of the computed mean of S_{6He} resulting values of about 10^{-3}, 10^{-4}, 10^{-5}, respectively for equatorial emission and 10^{-7}, 10^{-8}, and 10^{-9}, respectively for collinear emission. As a result, raising the excitation energy of stage (I) by 1 MeV reduces the order of the preformation probability by a factor of one. The greatest known excitation energy of the A_1 fragments participating in the explored ^{6}He channels spans from 2.737 MeV ($^{156}Nd(16^+)$) to 7.566 MeV ($^{134}Te(15^+)$). Columns 3(6) and 4(7) of Table II list the computed mean relative yields and the estimated mean preformation probabilities with excitation energy of preceding step (I) E^*_I = 3 MeV, equivalent to E^*_{A1}= 1.5 MeV and E^*_{ACN23} = 1.5 MeV, and E^*_I = 4 MeV, equivalent to E^*_{A1} = 2 MeV and E^*_{ACN23} = 2 MeV, for the ^{6}He-accompanied ternary fission channels of ^{252}Cf based on collinear and equatorial ternary fission configurations respectively. For the collinear emission (Q_{23} = 6.15 MeV), the extracted values of S^{ave}_{6He} (E^*_I = 3-4 MeV) lies between 2.41×10^{-11} and 6.82×10^{-7}, with an average value of 1.11×10^{-7}. For the equatorial emission (Q_{23} = 12.3 MeV), the S^{ave}_{6He} (E^*_I = 3-4 MeV) values range from 2.86×10^{-6} to 1.79×10^{-3}, with a mean value of 2.69×10^{-4}. These E^*_I values represent the optimal excitation energy of the identical heaviest fragments involved in the ^{4}He channels.

Furthermore, A_3 = 10 and A_3 = 14 ternary breakup channels of ^{252}Cf were detected using ^{10}Be and ^{14}C as emitted light nuclei, respectively. Table II lists these channels and their relative experimental yields. The greatest relative experimental yields of 0.054% and 0.040% were reported for the ternary fission channels (^{136}Te + ^{106}Mo + ^{10}Be) and (^{132}Sn + ^{106}Mo + ^{14}C) respectively. The kinetic energies of the released ^{10}Be and ^{14}C nuclei at the maximal estimated yield is approximately 18.8 MeV and 26.0 MeV respectively. Figures 5(a) and 5(b) display the dependence of the logarithm of the preformation probability of ^{10}Be and ^{14}C nuclei (log (S_{10Be}) and log (S_{14C})) on the heaviest nucleus mass number (A_1) for the ^{10}Be and ^{14}C accompanied ternary fission channels of ^{252}Cf in collinear configuration, evaluated for different excitation energies of step (I) E^*_I (E^*_{A1}, E^*_{ACN23}) = 1 − 7 MeV with Q_{23} = 0.5 KE_{3exp} = 9.9 MeV and 13 MeV respectively. In Fig. (5), continuous, dashed, and dotted curves are used to draw the viewer's attention. As seen in Fig. (5), increasing the excitation energy E^*_I (E^*_{A1}, E^*_{ACN23}) lowers the anticipated preformation probability values. The mean relative yields estimated at excitation energies E^*_I = 3 and 4

MeV for the ^{10}Be and ^{14}C accompanied ternary breakup channels, their experimental relative yields as well as their related mean preformation probabilities derived from these computations are listed in Table II. For the ^{10}Be (^{14}C) collinear emission (Q_{23} = 9.9 (13) MeV), the extracted values of $S^{ave}{}_{10Be(14C)}$ (E^*_I = 3 - 4 MeV) lies between $7.44 \times 10^{-26}(3.13 \times 10^{-37})$ and $1.72 \times 10^{-18}(2.17 \times 10^{-29})$, with an average value of $2.13 \times 10^{-19}(3.96 \times 10^{-30})$. For the ^{10}Be (^{14}C) equatorial emission (Q_{23} = 18.8 (26) MeV), the $S^{ave}{}_{10Be(14C)}$ (E^*_I = 3 - 4 MeV) values range from $1.98 \times 10^{-15}(1.22 \times 10^{-23})$ to $1.30 \times 10^{-13}(2.45 \times 10^{-22})$, with a mean value of $2.94 \times 10^{-14}(9.60 \times 10^{-23})$. The findings shown in Fig. 5 and Table II imply that the preformation probability of the released light nucleus falls dramatically as the mass number increases.

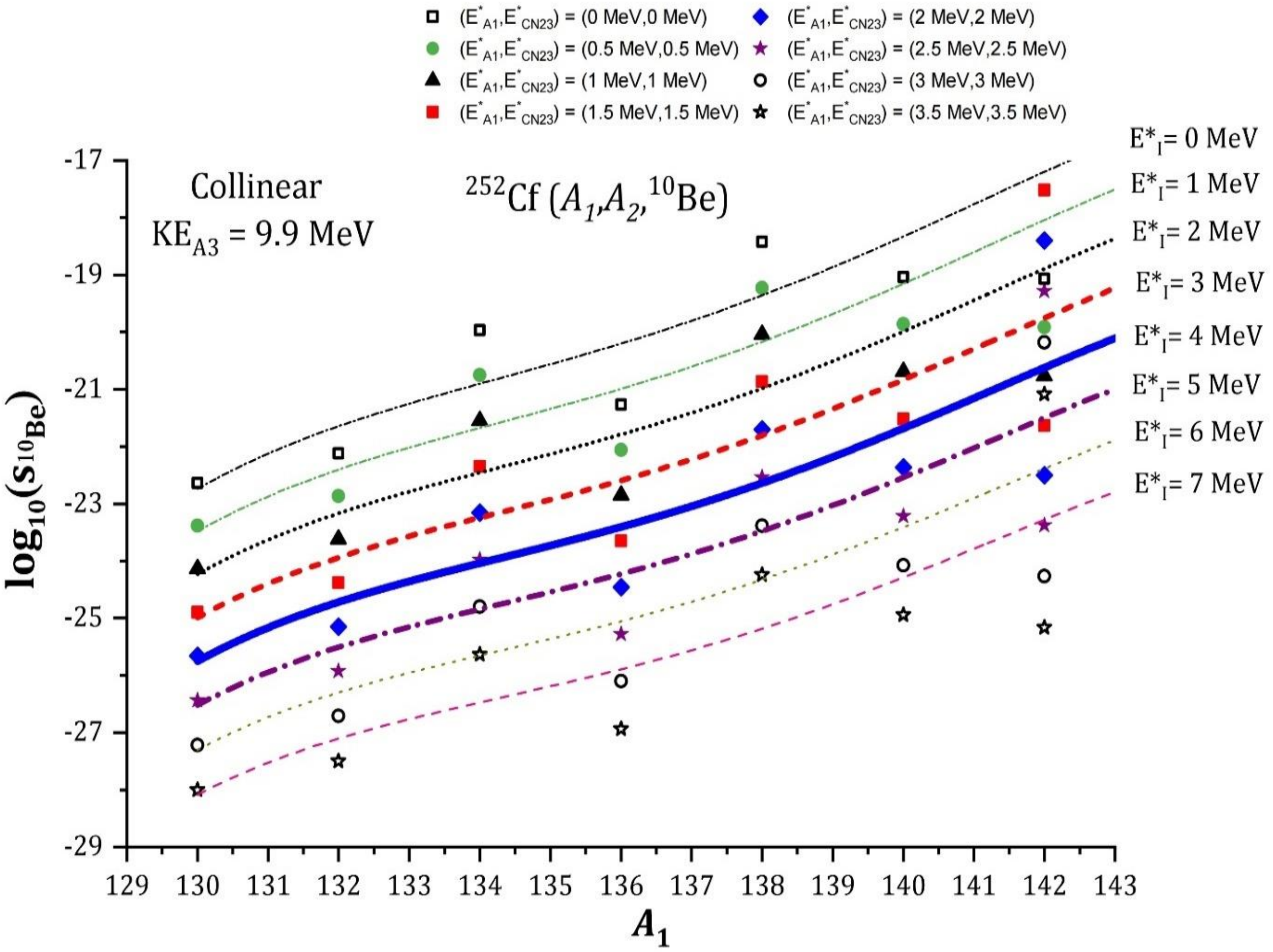

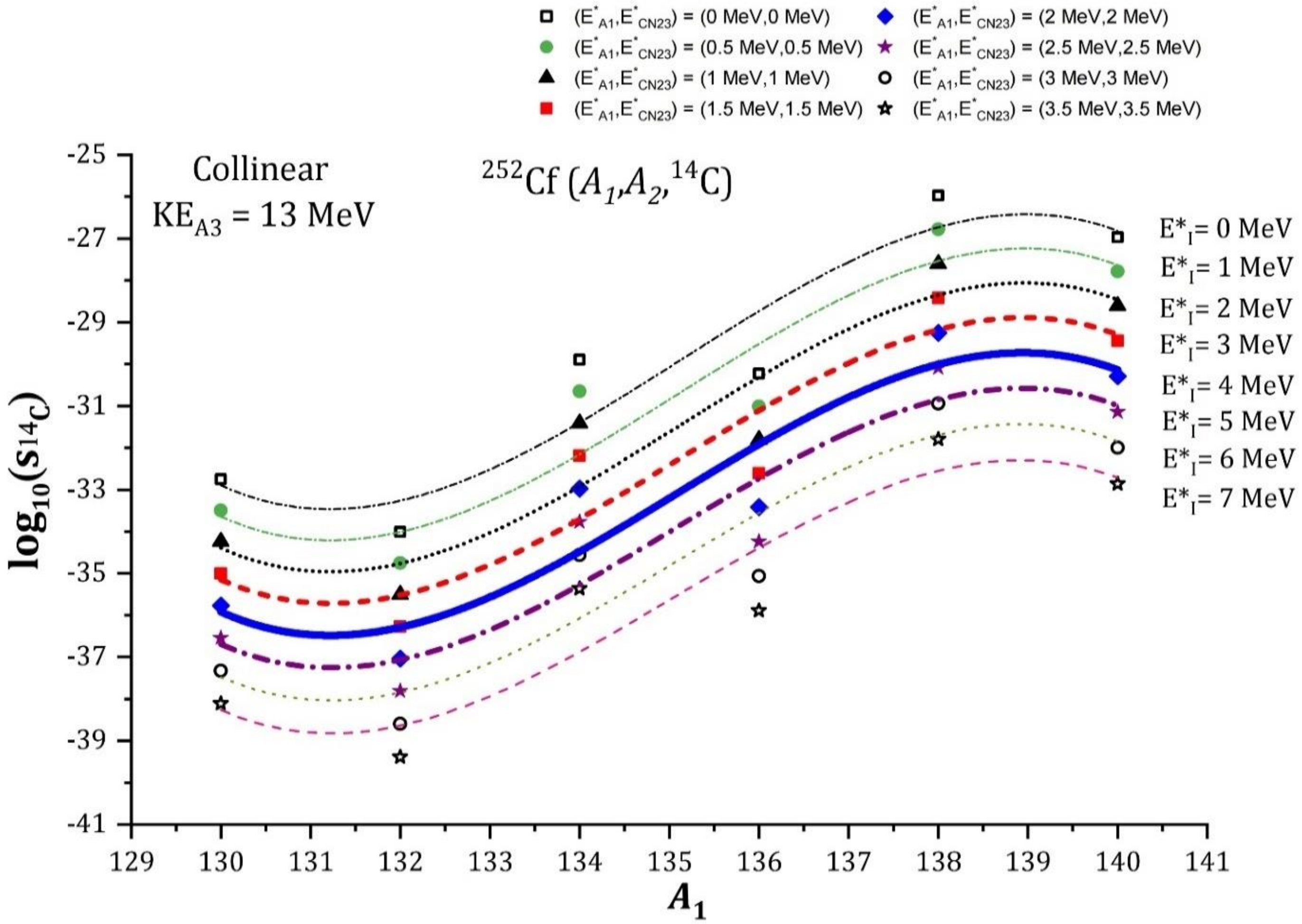

Fig. 5: Same as Fig. 4 but for the (a) ^{10}Be with Q_{23} = 9.9 MeV and (b) ^{14}C with Q_{23} = 13 MeV accompanied-^{252}Cf ternary fission channels.

Figure 6 illustrates the expected mean preformation probability versus the mass number A_3, as determined by computations done at E^*_I (E^*_{A1}, E^*_{ACN23}) = 2 - 5 MeV for the various ternary fragmentations shown in Tables I and II based on collinear configuration of the fragments. Fig. (6) indicates that $S_c(A_3)$ falls exponentially as the mass number A_3 increases. Figure 6 depicts a less diminishing pattern of $S_c(A_3)$ with E^*_I. The mean values of $S_c(A_3)$ determined by taking into account the various channels at the optimal excitation energy of E^*_I = 3 and 4 MeV based on collinear configuration of the fragments may be fitted in terms of A_3 as

$$S_c(collinear) = 2.69 \times 10^7 e^{-6.05\,A_3}. \qquad (20)$$

While the corresponding fitted formula based on equatorial configuration **[44]** of the fragments is given as

$$S_c(equatorial) = 10^7 e^{-4.8\,A_3}. \qquad (21)$$

The open circles in Fig. (6) indicate the preformation probability if estimated utilizing the descriptive equation defined by Eq (20). The dimensionless factors -6.05 and -4.8 in the exponent of equations (20) and (21) indicate the exponentially decaying constants of the preformation probability (S_c) in terms of A_3.

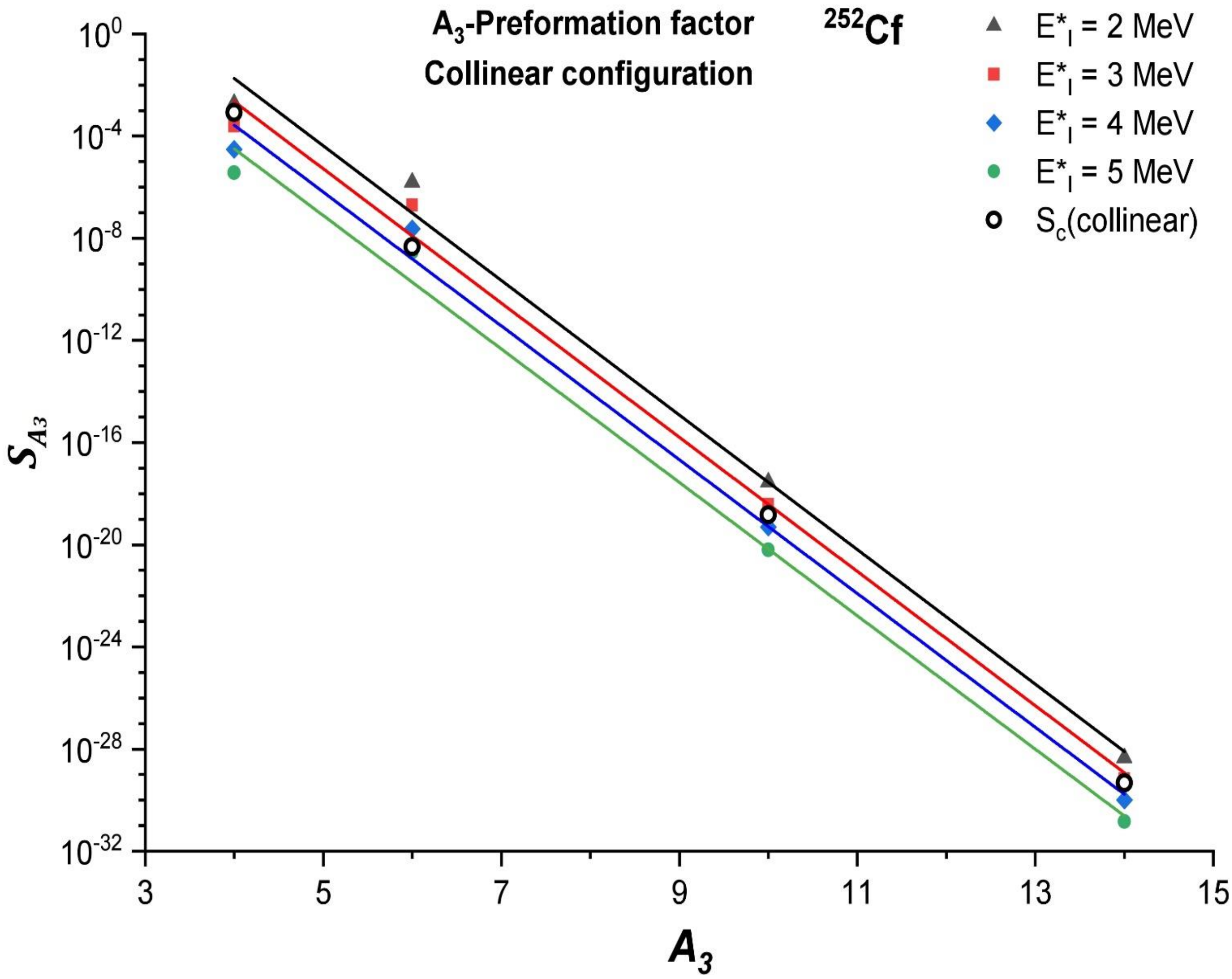

Fig. 6: Mean preformation probability versus the light nucleus mass number A_3, as determined from the computations executed at E^*_I (E^*_{A1}, E^*_{ACN23}) = 2 − 5 MeV for the various ^{4,6}He, ^{10}Be and ^{14}C accompanied ternary fission channels of ^{252}Cf in collinear configuration (shown in Tables I and II). The open circles represent the preformation probabilities calculated by (S_c: Eq.20).

Table II: The mean calculated relative yield Y^{ave}_{cal} and the obtained mean preformation probability S^{ave}_{c} taking into consideration the optimized excitation energy E^{*}_{I} (E^{*}_{A1}, E^{*}_{ACN23}) = 3 and 4 MeV, for the released ^{6}He, ^{10}Be and ^{14}C ternary fission channels of ^{252}Cf based on collinear (Q_{23} = 0.5 KE_c) and equatorial (Q_{23} = KE_c) arrangements of the ternary system. The experimental relative yields, as well as the preformation probability calculated using the phenomenological formula given by Eqs. (20) and (21) for collinear and equatorial configurations respectively, are also reported.

Ternary fission Channel	Y_{exp}	Collinear ($Q_{23} = 0.5KE_c$)			Equatorial ($Q_{23} = KE_c$) [44]		
		Y^{ave}_{cal}	S^{ave}_{cal}	S_c (Eq. 20)	Y^{ave}_{cal}	S^{ave}_{cal}	S_c (Eq. 21)
^{156}Nd+^{90}Kr+^{6}He	8.00×10^{-3}	2.09×10^{-9}	2.62×10^{-7}	4.70×10^{-9}	7.53×10^{-6}	4.70×10^{-4}	3.11×10^{-6}
^{154}Nd+^{92}Kr+^{6}He	3.60×10^{-3}	2.16×10^{-9}	6.00×10^{-7}		7.35×10^{-6}	1.79×10^{-3}	
^{150}Ce+^{96}Sr+^{6}He	2.10×10^{-2}	3.40×10^{-10}	1.62×10^{-8}		4.38×10^{-6}	4.51×10^{-4}	
^{148}Ce+^{98}Sr+^{6}He	4.90×10^{-3}	3.69×10^{-10}	7.53×10^{-8}		3.55×10^{-6}	9.35×10^{-4}	
^{146}Ce+^{100}Sr+^{6}He	5.30×10^{-4}	3.61×10^{-10}	6.82×10^{-7}		1.19×10^{-6}	3.96×10^{-5}	
^{146}Ba+^{100}Zr+^{6}He	1.00×10^{-2}	5.49×10^{-11}	5.49×10^{-9}		1.07×10^{-6}	5.65×10^{-5}	
^{144}Ba+^{102}Zr+^{6}He	1.30×10^{-2}	6.70×10^{-11}	5.16×10^{-9}		8.71×10^{-7}	6.22×10^{-5}	
^{142}Ba+^{104}Zr+^{6}He	5.30×10^{-3}	7.41×10^{-11}	1.40×10^{-8}		2.75×10^{-7}	5.20×10^{-5}	
^{142}Xe+^{104}Mo+^{6}He	1.40×10^{-2}	8.58×10^{-12}	6.13×10^{-10}		2.75×10^{-7}	2.11×10^{-5}	
^{140}Xe+^{106}Mo+^{6}He	1.90×10^{-2}	1.17×10^{-11}	6.18×10^{-10}		2.47×10^{-7}	2.47×10^{-5}	
^{138}Xe+^{108}Mo+^{6}He	3.00×10^{-2}	1.44×10^{-11}	4.79×10^{-10}		5.35×10^{-8}	1.01×10^{-4}	
^{136}Te+^{110}Ru+^{6}He	3.80×10^{-3}	1.96×10^{-12}	5.17×10^{-10}		5.99×10^{-8}	1.22×10^{-5}	
^{134}Te+^{112}Ru+^{6}He	9.70×10^{-3}	2.70×10^{-12}	2.78×10^{-10}		6.00×10^{-8}	2.86×10^{-6}	
^{132}Sn+^{114}Pd+^{6}He	4.10×10^{-3}	3.36×10^{-13}	8.20×10^{-11}		4.43×10^{-8}	1.23×10^{-5}	
^{130}Sn+^{116}Pd+^{6}He	1.60×10^{-2}	3.85×10^{-13}	2.41×10^{-11}		4.70×10^{-8}	5.87×10^{-6}	
^{146}Ba+^{96}Sr+^{10}Be	8.30×10^{-4}	2.75×10^{-22}	3.31×10^{-19}	1.47×10^{-19}	1.95×10^{-16}	1.30×10^{-14}	1.43×10^{-14}
^{144}Ba+^{98}Sr+^{10}Be	4.60×10^{-3}	3.54×10^{-22}	7.71×10^{-20}		1.92×10^{-16}	5.05×10^{-14}	
^{142}Ba+^{100}Sr+^{10}Be	2.40×10^{-4}	4.13×10^{-22}	1.72×10^{-18}		1.39×10^{-16}	4.35×10^{-14}	
^{142}Xe+^{100}Zr+^{10}Be	2.70×10^{-2}	3.59×10^{-24}	1.33×10^{-22}		1.15×10^{-16}	2.13×10^{-15}	
^{140}Xe+^{102}Zr+^{10}Be	3.00×10^{-2}	5.16×10^{-24}	1.72×10^{-22}		6.98×10^{-17}	8.11×10^{-15}	
^{138}Xe+^{104}Zr+^{10}Be	8.60×10^{-3}	6.67×10^{-24}	7.75×10^{-22}		6.45×10^{-17}	2.15×10^{-15}	
^{136}Te+^{106}Mo+^{10}Be	5.40×10^{-2}	6.96×10^{-26}	1.29×10^{-24}		5.35×10^{-17}	1.98×10^{-15}	
^{134}Te+^{108}Mo+^{10}Be	3.20×10^{-3}	8.26×10^{-26}	2.58×10^{-23}		3.13×10^{-17}	1.30×10^{-13}	
^{132}Sn+^{110}Ru+^{10}Be	3.80×10^{-3}	9.25×10^{-28}	2.43×10^{-25}		3.22×10^{-17}	6.99×10^{-15}	
^{130}Sn+^{112}Ru+^{10}Be	1.50×10^{-2}	1.12×10^{-27}	7.44×10^{-26}		2.98×10^{-17}	3.60×10^{-14}	
^{140}Xe+^{98}Sr+^{14}C	3.50×10^{-3}	7.15×10^{-33}	2.04×10^{-30}	4.60×10^{-30}	4.96×10^{-25}	1.84×10^{-22}	6.54×10^{-23}
^{138}Xe+^{100}Sr+^{14}C	4.40×10^{-4}	9.54×10^{-33}	2.17×10^{-29}		4.89×10^{-25}	1.22×10^{-23}	
^{136}Te+^{102}Zr+^{14}C	6.90×10^{-3}	9.73×10^{-36}	1.41×10^{-33}		2.85×10^{-25}	7.31×10^{-23}	
^{134}Te+^{104}Zr+^{14}C	3.90×10^{-3}	1.45×10^{-35}	3.73×10^{-33}		2.35×10^{-25}	3.41×10^{-23}	
^{132}Sn+^{106}Mo+^{14}C	4.00×10^{-2}	1.25×10^{-38}	3.13×10^{-37}		1.08×10^{-25}	2.45×10^{-22}	
^{130}Sn+^{108}Mo+^{14}C	2.70×10^{-3}	1.56×10^{-38}	5.78×10^{-36}		9.98×10^{-26}	2.85×10^{-23}	

4. Conclusion

The collinear cluster tripartition kinematics were utilized to investigate the preformation probability of the light clusters $^{4,6}He$, ^{10}Be, and ^{14}C released in the accompanied ternary fission channels of ^{252}Cf. The estimated preformation probabilities are compared to those obtained by the previously used equatorial configuration. The light nucleus in collinear configuration is most likely grouped with a specified preformation probability inside the intermediate compound nucleus A_{CN23}. The probability of formation of the light nucleus was assessed by dividing the computed relative yield by the measured experimental yield. According to the calculations, the optimal excitation energy of the heaviest nucleus participating in the ternary fission reaction that contains α-particle is around three and four MeV. The predicted preformation probability of α-particles in their accompanied ternary fission channels spans from 10^{-3} to 10^{-5} and from 10^{-1} to 10^{-3} based on collinear and equatorial configurations respectively. It has been discovered that raising the excitation energy E^*_I reduces the predicted relative yields and hence implying a lower preformation probability. Raising the excitation energy of the preceding step (I) E^*_I by a value of 1 MeV reduces the predicted mean preformation probability by almost one order of magnitude. the predicted preformation probability of the released light clusters heavier than α-particles falls in an exponential way as the mass number increases. According to the achieved results, a qualitative equation for calculating the preformation probability of a particular released nucleus as a function of its mass number A_3 is proposed for collinear configuration. This equation will aid in the estimation and analysis of the possible heavy and superheavy nuclei ternary fission channels. In general, the collinear configuration produces a lower estimated yield and a lower probability of formation as compared to the equatorial arrangement. The collinear arrangement implies hindrance in both predicted yield and preformation probability as compared to the corresponding equatorial arrangement. The collinear configuration is more preferred for ternary fission accompanying heavy third fragments.

References

[1] Poenaru, D N, Greiner, W, Hamilton, J H, Ramayya, A V, Hourany, E, & Gherghescu, R A, "Multicluster accompanied fission", Phys. Rev. C 59(6), 3457, (1999).

[2] Poenaru, D N, Dobrescu, B, Greiner, W, Hamilton, J H, & Ramayya, A V, "Nuclear quasi-molecular states in ternary fission", J. Phys. G: Nuclear and Particle Physics 26, L97, (2000).

[3] Zagrebaev, V I, Karpov, A V, & Greiner, W, "True ternary fission of superheavy nuclei", Phys. Rev. C 81, 044608, (2010).

[4] Pyatkov, Y V, et al., Rom. Rep. Phys 59, 569–582, (2005).

[5] Pyatkov, Y V, et al. "Collinear cluster tri-partition of ^{252}Cf (sf) and in the ^{235}U (nth, f) reaction", Eur. Phys. J. A 45, 29-37, (2010).

[6] Pyatkov, Y V, et al. "The collinear cluster tri-partition (CCT) of ^{252}Cf (sf): New aspects from neutron gated data", Eur. Phys. J. A 48, 1-16, (2012).

[7] Nasirov, A K, von Oertzen, W, Muminov, A I, & Tashkhodjaev, R B, "Peculiarities of cluster formation in true ternary fission of ^{252}Cf and 236U", Phys. Scripta 89, 054022, (2014).

[8] Von Oertzen, W, Nasirov, A K, & Tashkhodjaev, R B, "Multi-modal fission in collinear ternary cluster decay of 252Cf (sf, fff) ", Phys. Lett. B 746, 223-229, (2015).

[9] Von Oertzen, W, Pyatkov, Y V, & Kamanin, D, "TRUE TERNARY FISSION, COLLINEAR CLUSTER TRI (CCT) PARTITION OF ^{252}Cf", Acta. Phys. Pol. B 44, (2013).

[10] Manimaran, K, & Balasubramaniam, M, "All possible ternary fragmentations of ^{252}Cf in collinear configuration", Phys. Rev. C 83, 034609, (2011).

[11] Santhosh, K P, Krishnan, S, & Priyanka, B, ^{34}Si accompanied ternary fission of ^{242}Cm in equatorial and collinear configuration. Int. J. Mod. Phys. E 23, 1450071, (2014).

[12] Hamilton, J H, et al. "New cold and ultra hot binary and cold ternary spontaneous fission modes for ^{252}Cf and new band structures with gammasphere", Prog. Part. Nucl. Phys 38, 273-287, (1997).

[13] Ramayya, A V, et al. "Cold (neutronless) α ternary fission of ^{252}Cf", Phys. Rev. C 57, 2370, (1998).

[14] Ramayya, A V, Hamilton, J H and Hwang, J K, "Binary and ternary spontaneous fission in ^{252}Cf", Rom. Rep. of Phys 59, 595, (2007).

[15] Wagemans, C, The nuclear fission process, CRC press, (1991).

[16] Vermote, S, Wagemans, C, Serot, O, Heyse, J, Van Gils, J, Soldner, T, & Geltenbort, P, "Ternary α and triton emission in the spontaneous fission of ^{244}Cm, ^{246}Cm and ^{248}Cm and in the neutron induced fission of ^{243}Cm, ^{245}Cm and ^{247}Cm. Nucl. Phys. A 806, 1-14, (2008).

[17] Hwang, J K, et al. "Search for scission neutrons in the spontaneous fission of ^{252}Cf", Phys. Rev. C

60, 044616, (1999).
[18] Singer, P, Kopatch, Y N, Mutterer, M, Klemens, M, Hotzel, A, Schwalm, D, Thirolf, P, & Hesse, M, Proceedings of the 3rd international conference on dynamical aspects of nuclear fission, Casta Papiernica, Slovakia, 262, (1996).
[19] Ismail, M, Seif, W M, Ellithi, A Y, & Hashem, A S, "(A= 10)-Accompanied spontaneous ternary fission of californium isotopes", Can. J. Phys. 91, 401-410, (2013).
[20] Kopatch, Yu N, et al. "^{5}He, ^{7}He, and ^{8}Li (E* = 2.26 MeV) intermediate ternary particles in the spontaneous fission of ^{252}Cf", Phys. Rev. C 65, 044614, (2002).
[21] Daniel, A V, et al. "Ternary fission of ^{252}Cf: 3368 keV γ radiation from ^{10}Be fragments", Phys. Rev. C 69, 041305 (2004).
[22] Ismail, M, Seif, W M, Hashem, A S, Botros, M M, & Abdul-Magead, I A M, "Ternary fission of ^{260}No in collinear configuration", Ann. of Phys, 372, 375-391, (2016).
[23] Ismail, M, Seif, W M, Hashem, A S, "Ternary fission of ^{260}No in equatorial configuration", Eur. Phys. J. A 52, 317, (2016).
[24] Farwell, G, Segrè, Emilio and Wiegand, C, "Long range alpha-particles emitted in connection with fission Preliminary report", Phys. Rev. 71, 327, (1947).
[25] Ter-Akopian, G M, et al., In proceedings of 3rd international conference fission and properties of neutron-rich nuclei, World Scientific, Singapore, 535, (2003).
[26] Herbach, C M, et al., Nucl. Phys. A 712, 207, (2002).
[27] Theobald, J P, Heeg, P, and Mutterer, M, Nucl. Phys. A 502, 343, (1989).
[28] Theobald, J P, Ph.D. Thesis, “Technische Hochschule Darmstadt”, TH Darmstadt, FRG, (1985).
[29] Vijayaraghavan, K R, von Oertzen, W, and Balasubramaniam, M, "Kinetic energies of cluster fragments in ternary fission of ^{252}Cf", Eur. Phys. J. A 48, 27, (2012).
[30] Holmvall, P, Köster, U, Heinz, A, and Nilsson, T, "Collinear cluster tri-partition: Kinematics constraints and stability of collinearity", Phys. Rev. C 95, 014602, (2017).
[31] Vautherin, D, Brink, D M, "Hartree-Fock calculations with Skyrme's interaction. I. Spherical nuclei", Phys. Rev. C 5, 626, (1972).
[32] Brack, M, Guet, C, Hakanson, H-B, "Selfconsistent semiclassical description of average nuclear properties - a link between microscopic and macroscopic models", Phys. Rep. 123, 275, (1985).
[33] Bartel, J, & Bencheikh, K, "Nuclear mean fields through self-consistent semiclassical calculations", Eur. Phys. J. A 14, 179, (2002).
[34] Bonche, P, Flocard, H, Heenen, P H, "Self-consistent calculation of nuclear rotations: The complete yrast line of ^{24}Mg.", Nucl. Phys. A 467, 115, (1987).
[35] Chabanat, E, Bonche, E, Haensel, E, Meyer, J, and Schaeffer, R, "A Skyrme parametrization from

subnuclear to neutron star densities Part II. Nuclei far from stabilities", Nucl. Phys. A 635, 231, (1998).

[36] Slater, J C, "A simplification of the Hartree-Fock method", Phys. Rev 81, 385, (1951).

[37] Titin-Schnaider, C and Quentin, P h, "Deformed Hartree-Fock calculations not restricted to very short range effective interactions", Phys. Lett. B 49, 213, (1974).

[38] Seif, W M, and Mansour, H, "Systematics of nucleon density distributions and neutron skin of nuclei", Int. J. Mod. Phys. E 24, 1550083, (2015).

[39] Buck, B, Merchant, A C, and Perez, S M, "α decay calculations with a realistic potential", Phys. Rev. C, 45, 2247, (1992).

[40] Buck, B, Merchant, A C, and Perez, S M, "Alpha-cluster structure in ^{212}Po.", Phys. Rev. Lett. 72, 1326, (1994).

[41] Buck, B, Johnston, J C, Merchant, A C, and Perez, S M, "Cluster model of α decay and ^{212}Po", Phys. Rev. C 53, 2841, (1996).

[42] Gurvitz, S A, and Kalbermann, G, "Decay width and the shift of a quasistationary state", Phys. Rev. Lett 59, 262, (1987).

[43] Kelkar, N G, and Castãneda, H M, "Critical view of WKB decay widths", Phys. Rev. C 76, 064605, (2007).

[44] Seif, W M, and Hashem, A S, "Preformation probability of light charged particles emitted equatorially in ternary fission of ^{252}Cf ", Phys. Rev. C 104, 014616, (2021).

[45] Ramayya, A V, et al., "Binary and ternary fission studies with ^{252}Cf", Prog. Part. Nucl. Phys. 46, 221, (2001).

[46] NuDat2.7, Nuclear Structure and Decay Data, http://www.nndc.bnl.gov/nudat2/.

[47] Audi, G, Kondev, F G, Wang, Meng, Huang, W J, Naimi, S, "The NUBASE2016 evaluation of nuclear properties", Chin. Phys. C 41, 030001, (2017).